www.czasopisma.pan.pl PAN www.journals.pan.pl

ARCHIVES of FOUNDRY ENGINEERING

ISSN (2299-2944)
Volume 2020
Issue 2/2020

53 – 58

9/2

10.24425/afe.2020.131302

Published quarterly as the organ of the Foundry Commission of the Polish Academy of Sciences

The Comparative Analysis of the Inclusion Removal Efficiency of Different Fluxes

M. Máté, M. Tokár, G. Fegyverneki, G. Gyarmati *
University of Miskolc, Institute of Metallurgy and Foundry Engineering, Department of Foundry
3515 Miskolc-Egyetemváros B/1 III, Hungary
* Corresponding author. E-mail address: gygabor007@gmail.com

Received 26.10.2019; accepted in revised form 14.01.2020

Abstract

The removal of inclusions is a major challenge prior to the casting process, as they cause a discontinuity in the cast material, thereby lowering its mechanical properties and have a negative impact on the feeding capability and fluidity of the liquid alloys. In order to achieve adequate melt quality for casting, it is important to clean the melts from inclusions, for which there are numerous methods that can be used. In the course of the presented research, the inclusion removal efficiency of rotary degassing coupled with the addition of different fluxes was investigated. The effects of various cleaning fluxes on the inclusion content and the susceptibility to pore formation were compared by the investigation of K-mold samples and the evaluation of Density Index values at different stages of melt preparation. The chemical composition of the applied fluxes was characterized by X-ray powder diffraction, while the melting temperature of the fluxes was evaluated by derivatographic measurements. It was found that only the solute hydrogen content of the liquid metal could be significantly reduced during the melt treatments, however, better inclusion removal efficiency could be achieved with fluxes that have a low melting temperature.

Keywords: Castings defects, Aluminum alloy, Inclusions, Cleaning flux, Melt treatment

1. Introduction

Inclusions are structural discontinuities inside the material which are mostly non-metallic or in some cases intermetallic phases embedded in a metallic matrix. Inclusions are distinct phases in molten alloys, which can occur in the form of solid particles, films or liquid droplets. The inclusions in aluminum alloys are usually non-metallic compounds like oxides, nitrides, carbides, and borides [1-4]. The most frequently occurring of all inclusions are the so-called double oxide films or bifilms, which can easily form due to any disturbance of the surface oxide layer of aluminum alloy melts. Bifilm formation is usually inevitable during common foundry activities like melting, alloying, fluxing and pouring, which is the main reason why these defects are the most common inclusions of light alloy melts [5-8]. Non-metallic inclusions based on their origin can be exogenous or indigenous. The formation of exogenous ones includes the entrainment of materials from external sources, for example, pieces of refractories and molding materials, or contaminations of the charge material (decomposition products of paints, oils, etc.). The other group includes reactions products formed in-situ in the molten alloy, like oxides, nitrides, and carbides [2]. The removal of inclusions is crucially important, as they reduce the mechanical properties (like tensile and fatigue properties) of cast parts and negatively affect melt fluidity and feeding capability of the molten alloy [4, 9, 10].

A further issue related to melt quality is the solute hydrogen content of the melt, which can result in porosity formation. Upon exposure, the humidity of the air reacts with the melt (Eq. 1):

$$2Al + 3H_2O = Al_2O_3 + 6H \quad (1)$$

The hydrogen released upon the formation of the aluminum-oxide is immediately dissolved as atomic hydrogen. In this way, the formation of aluminum-oxide and the increment of solute hydrogen content can take place simultaneously [11, 12].

There are numerous melt treatment methods that can improve the cleanliness of the molten metal, from which rotary degassing is the most commonly used technique in the foundry industry [13]. During rotary degassing, inert (Ar) or quasi-inert (N_2) gas is introduced into the liquid metal through a rotating impeller, which grants evenly distributed, small-sized purging gas bubbles. These bubbles can efficiently collect solute hydrogen through the diffusion of hydrogen atoms into their inner atmosphere, where the hydrogen atoms precipitate as H_2 gas. During the rise of the purging gas bubbles, the entrained inclusions can be removed from the liquid metal by the additional buoyancy provided by the gas bubbles colliding with them. As it is shown in Fig. 1, rotary degassing can be coupled with flux addition which can greatly increase the inclusion removal efficiency of the treatment [14, 15].

Fluxes are usually solid blends of inorganic compounds, which may serve several functions, such as the removal of non-metallic inclusions from the melt, the protection of the melt surface or the refinement and/or degassing of the molten alloy. The effectivity of fluxes is dependent on their chemical composition, morphology, added quantity, as well as the temperature of the melt and the method of flux addition. It is important that the compounds in the fluxes should have a lower density than the treated alloy and should be able to form low-melting high-fluidity mixtures at working temperatures [16, 17].

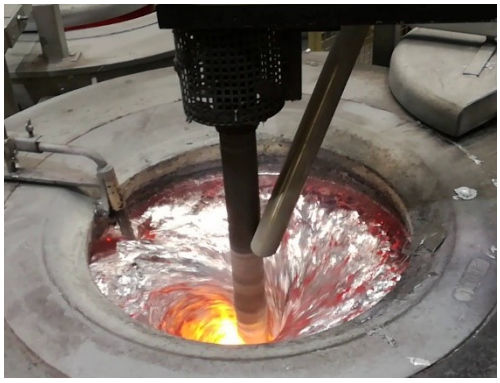

Fig. 1. Flux addition during rotary degassing

The base flux components can be classified into four major groups based on their primary influence on the mixture: chlorides, fluorides, solvents of aluminum oxides and oxidizing compounds. Chlorides are principally used for their fluidizing effect, and they are also used as filler and carrier materials. Fluoride compounds act as surfactants and wet the interface between the inclusions and the liquid metal. Consequently, fluorides promote inclusion separation and metal coalescence. Oxidizing compounds are applied to generate exothermic chemical reactions, which help the coalescence of larger aluminum droplets trapped in the dross layer. In this way, the recovery of useful metal is facilitated. On the other hand, the heat released during the reactions facilitates the interfacial reactions between the molten flux and the inclusions in the melt [16, 17].

2. Experimental

2.1. Melt treatment experiments

The aim of the presented research work was to compare the melt cleaning efficiency of 3 different commercially available cleaning fluxes (noted as A, B, and C), and to find a relationship between the properties of the fluxes and their inclusion removal efficiency. For this purpose, melt treatments involving rotary degassing with N_2 purging gas coupled with flux addition were executed on an Al-Si-Mg-Cu alloy. The chemical compositional ranges of the alloying elements of the investigated alloy are presented in Table 1.

Table 1.
Chemical composition of the studied aluminum alloy (wt%)

Si	Fe	Cu	Mn	Mg	Ti	Sr
6.5-7.5	<0.2	0.45-0.58	<0.1	0.36-0.45	<0.2	0.017-0.030

Each flux was used in 5 treatment cycles, the quantity of one portion of treated melt was approx. 1000 kg. The metal was melted in a stack smelter then was transported by a transport ladle to a resistance heated holding furnace where the melt treatments were performed. In each case, the melt was poured into a lesser quantity of melt (ca. 200 kg) which remained in the holding furnace from the previous cycle. The treatment parameters and the quantity of flux added (400 g) were the same in each cycle. The N_2 gas flow rate was 20 L/min; the rotor revolution was 490 RPM during vortex formation and 250 RPM in the degassing phase. The treatment time was 12 minutes in each case. The molten metal temperature in the holding furnace was maintained between 730 °C and 750 °C.

In order to get comprehensive information about the effect of the fluxes on the melt quality, different samples were taken at several stages of the melt preparation: specimens were cast from the melt in the transport ladle, from the liquid metal in the holding furnace before and after the melt treatments, and following a 15 minute long holding time. The inclusion content of the melts was studied by the visual examination of the fracture surfaces of K-mold samples. The K-mold specimen itself is a flat plate with four notches which act as fracture points (Fig. 2).

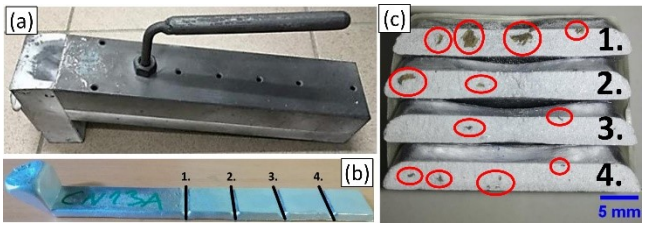

Fig. 2. (a) K-mold, (b) K-mold sample and (c) inclusions on the fracture surfaces

After the inclusions found on the fracture surfaces of a sample is counted, a K-value can be determined, that can be used for the quantitative characterization of the melt quality (Eq. 2):

$$K = \frac{S}{n} \quad (2)$$

where S is the number of inclusions and n is the number of fracture surfaces examined [4, 12]. For practical purposes, the melt quality can be classified based on the K-values, as it is presented in Table 2. During the experiments, 5 K-mold samples were cast in each sampling step.

Table 2.
Classification of melt quality based on K-values

Qualification	K-value	Melt quality
A	< 0.1	High melt quality
B	0.1 – 0.5	Good melt quality
C	0.5 – 1.0	Average melt quality
D1	1.0 – 2.0	Contaminated melt
D2	2.0 – 5.0	
D3	5.0 – 10	
E	> 10	Highly contaminated, bad melt quality

The effect of different fluxes on the melt purity was evaluated using the comparison of the K-values determined before and after the melt treatments. The percentage of change in K-values (ΔK [%]) was calculated using Eq. 3:

$$\Delta K = \frac{K_2 - K_1}{K_1} \cdot 100 \quad (3)$$

where K_1 is the K-value determined before the melt treatment and K_2 is the K-value determined after the melt processing. The inclusions found on the fracture surfaces were investigated with Zeiss EVO MA 10 scanning electron microscope (SEM) equipped with an energy-dispersive X-ray spectroscopy (EDS) system.

The susceptibility of the alloy to porosity formation was characterized by Density-Index evaluation. During this method, two samples are taken, one is allowed to solidify under atmospheric pressure while the other one solidifies in a vacuum chamber with a pressure of 80 mbar. Under reduced pressure, the solubility of hydrogen in the alloy is lowered, thus the H_2 precipitation process is during pore formation is accelerated [18]. On the other hand, during solidification under reduced pressure, the entrained air between the layers of double oxide films is expanded [8, 19]. As a result, pore formation in the samples is facilitated. Based on the density of the two samples the Density Index (DI) can be calculated (Eq. 4) which can be used for the quantitative characterization of susceptibility to pore formation:

$$DI = \frac{D_{atm} - D_{80mbar}}{D_{atm}} \cdot 100 \quad (4)$$

where DI is the Density-Index [%], D_{atm} is the density of the sample solidified under atmospheric pressure [g/cm^3] and D_{80mbar} is the density of the specimen solidified under 80 mbar [g/cm^3] [20]. Density-Index samples were cast before and following the melt treatments, as well as after the 15 minutes long holding period.

2.2. Flux characterization

The stereomicroscopic images of the applied fluxes are shown in Fig. 3. As can be seen, all fluxes are granular, with no significant difference in their average grain sizes. The chemical composition of the 3 different cleaning flux was investigated with Rigaku MiniFlexII Desktop X-ray Diffractometer (XRD). The melting temperature of the fluxes was investigated with derivatographic measurements. The derivatograph is capable of performing differential thermal analysis (DTA) and thermogravimetric (TG) measurements on the same sample at the same time. During the investigations, a MOM Derivatograph-C apparatus was used with a platinum crucible, the rate of heating was 10 °C/min, the maximum temperature of the measurement was 1000 °C. α-Al_2O_3 was used as reference material, the mass of each flux sample was 150 mg.

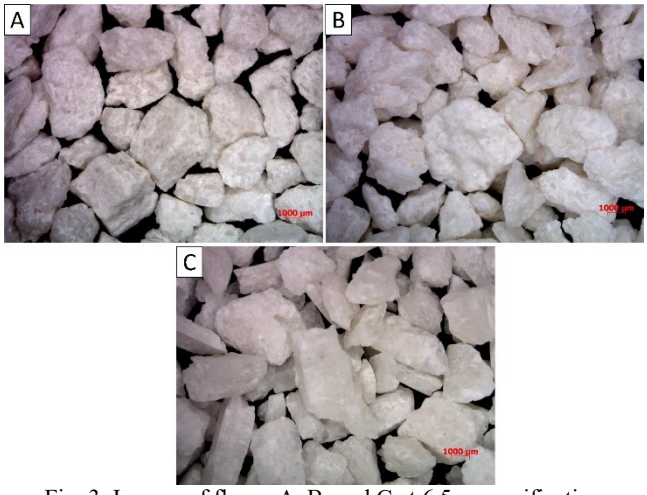

Fig. 3. Images of fluxes A, B, and C at 6.5x magnification

The evaluation process of the melting temperature from the measured data is described via the analysis of DTA, TG and DTG curves recorded during the investigation of flux B (Fig. 4.).

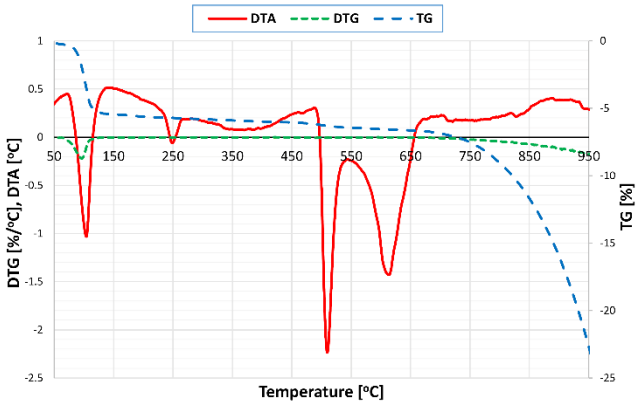

Fig. 4. The derivatographic curves of flux B

The DTA curve represents the temperature difference between the inert reference material and the flux sample during heating.

Negative peaks on the DTA curve indicate endothermic reactions while positive peaks are the signs of exothermic reactions. The TG curve gives information about the percentage of the mass change of the flux sample. The DTG curve is the first derivative of the TG curve with respect to temperature. In order to find the melting temperature of the flux, the temperature values where strongly endothermic reactions occur according to the DTA curve, but no mass-change can be observed on the DTG curve should be identified. In the case of flux B, two significantly endothermic reactions with no mass-change can be identified. The first one is around 510 °C and the second one is around 615 °C. The results indicate that the melting process of this flux starts at 510 °C, and the melting of another phase with a higher melting temperature takes place at 615 °C. With the aid of the described evaluation process, the melting temperature of each flux has been determined.

3. Results and discussion

The average K-values evaluated at different stages of melt preparation are shown in Fig. 5.

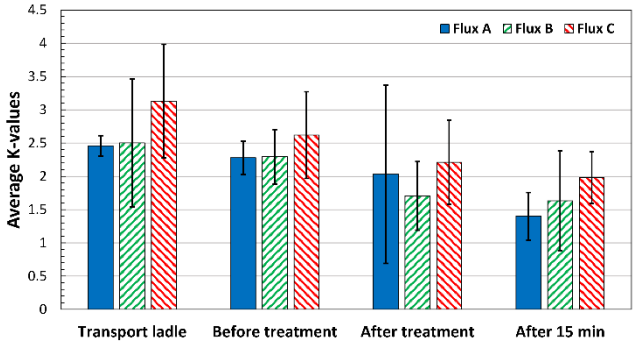

Fig. 5. Average K-values at different melt preparation stages

Based on the results shown in Fig. 5., optimal melt cleanliness could not be obtained during melt processing, even the lowest average K-values indicate contaminated melt (D1 quality in Table 2.). This means that the melt treatments had low inclusion removal efficiency in each case. The calculated ΔK values are -10.97 %, -25.61 % and -15.65 % in the case of fluxes A, B, and C, respectively. This clearly shows that treatments with flux B were the most effective regarding inclusion removal. Fig. 6. shows examples of inclusions found during the examination of K-mould samples. In most cases, creased film-like inclusions were found on the fracture surfaces, whose distinct layers could be distinguished on the opposing fracture surfaces, which confirms the theory that double oxide films (bifilms) are the most common inclusions of aluminum casting alloys [5].

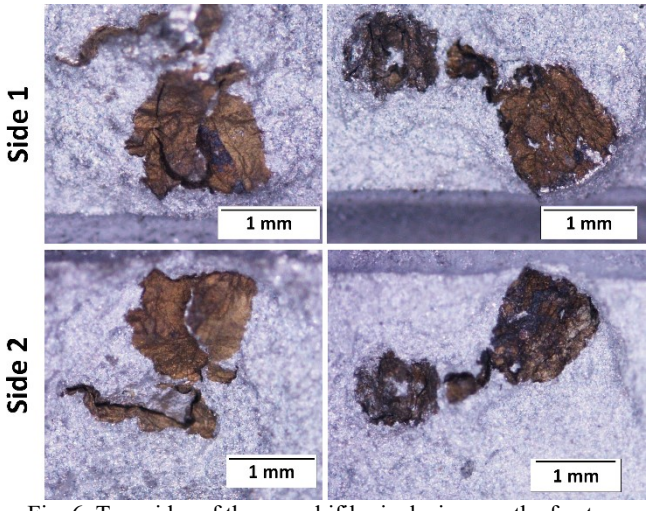

Fig. 6. Two sides of the same bifilm inclusions on the fracture surface of K-mold samples

Based on the EDS-SEM analysis, most found inclusions are oxide films, since the measured oxygen concentration was significantly high in each case. An example of the results of the SEM analysis of inclusions is shown in Fig. 7. The results of Density-Index evaluation are presented in Fig. 8.

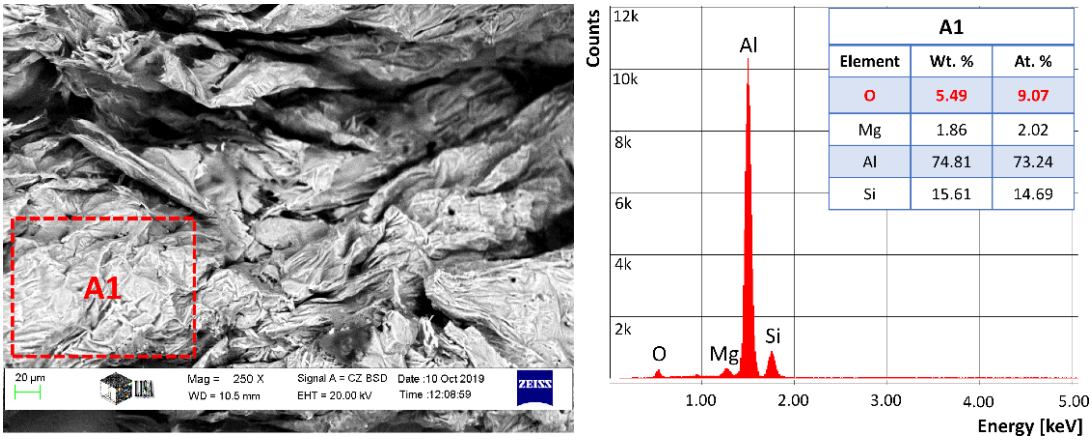

Fig. 7. SEM image of an oxide film inclusion with the results of EDS analysis on the indicated area

There was no significant difference between the DI values determined after the melt treatments, the melt treatments resulted in significantly lower DI results regardless of the flux used. This suggests that each melt treatment was efficient regarding solute hydrogen removal.

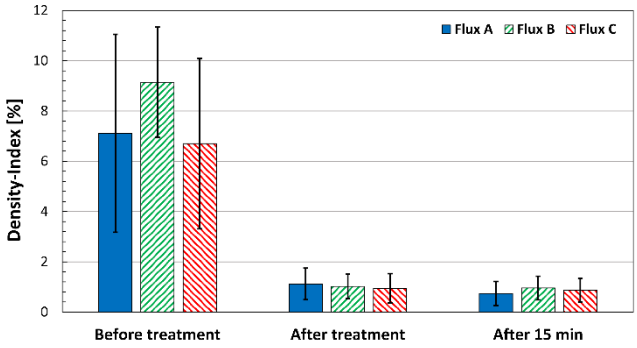

Fig. 8. Average Density-Index values

The results of the XRD analysis of the fluxes are shown in Fig. 9. Based on the X-ray diffraction patterns, the chemical composition of the three fluxes is similar, as they all contain NaCl, Na_2SO_4, and CaF_2. Besides that, flux B and C also have KCl which is commonly used together with NaCl as a carrier material, because they form a eutectic with a relatively low eutectic temperature of 657 °C [21], which provides low melting temperature to the mixture. In all fluxes, CaF_2 is used as a surfactant, which can alter interfacial energies between the inclusions, the molten flux and the liquid alloy [3, 16]. Na_2SO_4 serves as an oxidizing compound in the fluxes, as Na_2SO_4 reacts with molten Al according to the following exothermic reaction [22]:

$$3Na_2SO_4 + 8Al \rightarrow 3Na_2S + 4Al_2O_3 \quad (5)$$

The heat released during this reaction increases the fluidity of the molten flux inside the alloy melt, which facilitates the interfacial reaction between the surfactants of the flux and the inclusions [3, 16, 17].

The melting temperatures of the fluxes determined with derivatographic analysis are 559 °C, 512 °C and, 638 °C for fluxes A, B, and C, respectively. This means, that flux B has the lowest melting temperature, which can explain why flux B was the most efficient in inclusion removal. The ability to clean the molten metal from inclusions is highly dependent on the fluidity of the fluxes. The viscosity of molten fluxes is temperature-dependent, so at a constant temperature the viscosity of fluxes with lower melting points is lower and their fluidity is better. During melt treatments, the liquid fluxes with better fluidity can be dispersed more evenly in the alloy melt, which results in better melt cleaning efficiency [23].

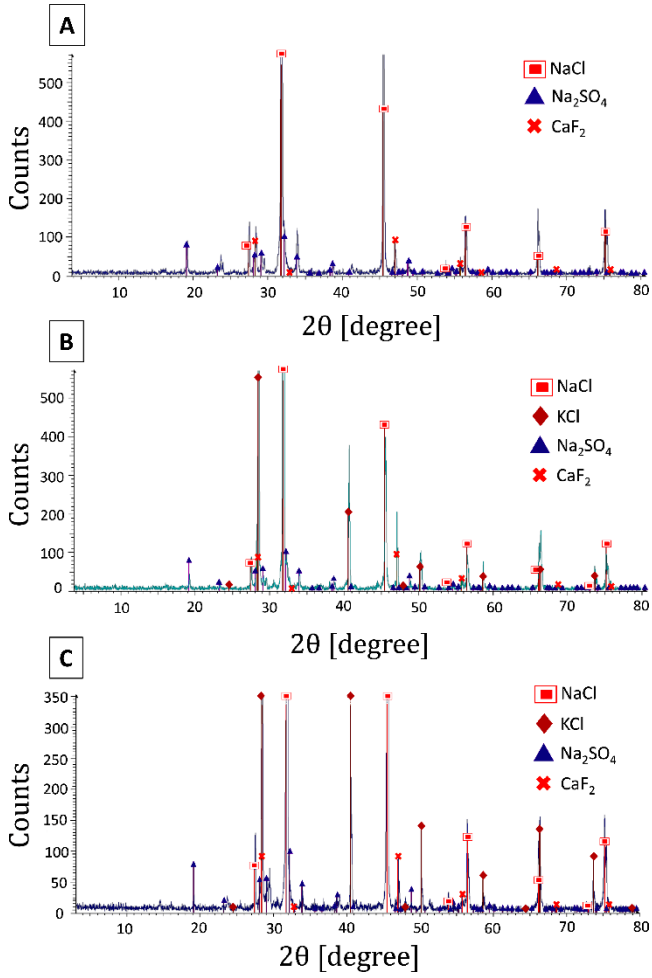

Fig. 9. X-ray diffraction pattern of fluxes A, B, and C

4. Conclusions

Based on the results of this study, the following conclusions can be drawn:

- only the solute hydrogen content of the melts could be significantly reduced during the rotary degassing and fluxing treatments,
- the average K-values indicate contaminated melts even after melt processing,
- the most common inclusions of aluminum casting alloys are double oxide films (bifilms),
- the melt cleaning efficiency of different fluxes is highly dependent on their physical and chemical properties,
- better inclusion removal efficiency can be achieved with fluxes which have a low melting temperature.

Acknowledgments

The described study was carried out as part of the EFOP-3.6.1-16-2016-00011 "Younger and Renewing University – Innovative Knowledge City – institutional development of the University of Miskolc aiming at intelligent specialization" project implemented in the framework of the Szechenyi 2020 program. The realization of this project is supported by the European Union, co-financed by the European Social Fund.

References

[1] Shivkumar, S., Wang, L., & Apelian, D. (1991). Molten metal processing of advanced cast aluminum alloys. *The Journal of The Minerals, Metals & Materials Society.* 43(1), 26-32. DOI: 10.1007/BF03220114.

[2] Trojan, P.K., & Fruehan, R. (2008). Inclusion-forming reactions. In *ASM Handbook.* 15*: Casting*, 74-83. ASM International. DOI: 10.1361/asmhba0005193.

[3] Gallo, R. (2017). "I Have Inclusions! Get Me the Cheapest and Best Flux for Cleaning My Melt" - Is This the Best Driven, Cost Saving Approach by a Foundry? *AFS Transactions.* 125, 97-110.

[4] Hudson, S.W., & Apelian, D. (2016). Inclusion detection in molten aluminum: current art and new avenues for in situ analysis. *International Journal of Metalcasting*. 10(3), 315-321. DOI: 10.1007/s40962-016-0030-x.

[5] Campbell, J. (2006). Entrainment defects. *Materials Science and Technology*. 22(2), 127-145. DOI: 10.1179/174328406 X74248.

[6] Cao, X., & Campbell, J. (2005). Oxide inclusion defects in Al-Si-Mg cast alloys. *Canadian Metallurgical Quarterly*. 44(4), 435-448. DOI: 10.1179/cmq.2005.44.4.435.

[7] Campbell, J. (2012). Stop pouring, start casting. *International Journal of Metalcasting.* 6(3), 7-18. DOI: 10.1007/BF03355529.

[8] Gyarmati, G., Fegyverneki, G., Mende, T., & Tokár, M. (2019). Characterization of the double oxide film content of liquid aluminum alloys by computed tomography. *Materials Characterization*. 157(109925). DOI: 10.1016/j.matchar. 2019.109925.

[9] Kaufman, J.G., & Rooy, E.L. (2004). The influence and control of porosity and inclusions in aluminum castings. In E. L. Rooy & J. G. Kaufman (Ed.), *Aluminum Alloy Castings: Properties, Processes, and Applications*. 47-54. ASM International. DOI: 10.1361/aacp2004p047.

[10] Cao, X.B., Zhao, J., Fan, J.H., Zhang, M.H., Shao, G.J., & Hua, Q. (2014). Influence of casting defects on fatigue behaviour of A356 aluminium alloy. *International Journal of Cast Metals Research.* 27(6), 362-368. DOI: 10.1179/ 1743133614Y.0000000120.

[11] Samuel, A.M., & Samuel, F.H. (1992). Various aspects involved in the production of low-hydrogen aluminium castings. *Journal of Materials Science.* 27(24), 6533-6563. DOI: 10.1007/BF01165936.

[12] Brůna, M., & Sládek, A. (2011). Hydrogen analysis and effect of filtration on final quality of castings from aluminium alloy AlSi7Mg0,3. *Archives of Foundry Engineering.* 11(1), 5-10.

[13] Czerwinski, F. (2017). Modern aspects of liquid metal engineering. *Metallurgical and Materials Transactions B.* 48(1), 367-393. DOI: 10.1007/s11663-016-0807-6.

[14] Brown, J.R. (1999). *Foseco Non-Ferrous Foundryman's Handbook*. (11th ed.) Oxford: Foseco International Ltd. 72-76.

[15] Neff, D.V. (2008). Degassing. In *ASM Handbook.* 15, *Casting*, 185-193. ASM International. DOI: 10.1361/ asmhba0005353.

[16] Utigard, T.A., Friesen, K., Roy, R.R., Lim, J., Silny, A., & Dupuis, C. (1998). The properties and uses of fluxes in molten aluminum processing. *Journal of The Minerals, Metals & Materials Society.* 50(11), 38-43. DOI: 10.1007/s11837-998-0285-7.

[17] Gallo, R. (2001). Development, Evaluation, and Application of Granular and Powder Fluxes in Transfer Ladles, Crucible, and Reverberatory Furnaces. In 6th International Conference on Molten Aluminum Processing, Nov. 2001 (pp. 55-69.) Orlando: American Foundry Society.

[18] DasGupta, R. (2008). Approaches to Measurement of Metal Quality. In *ASM Handbook.* 15, Casting, 1167-1173. ASM International. DOI: 10.31399/asm.hb.v15.a0005 340.

[19] Fox, S., & Campbell, J. (2000). Visualisation of oxide film defects during solidification of aluminium alloys. *Scripta Materialia.* 43, 881-886. DOI: 1016/S1359-6462(00)00506-6.

[20] Djurdjevic, M.B., Odanovic, Z., & Pavlovic-Krstic, J. (2010). Melt quality control at aluminium casting plants. *Metallurgical & Materials Engineering.* 16(1), 63-76.

[21] Li, C., Li, J., Mao, Y., & Ji, J. (2017). Mechanism to remove oxide inclusions from molten aluminum by solid fluxes refining method. *China Foundry.* 14(4), 233-243. DOI: 10.1007/s41230-017-7005-2.

[22] Ambrová, M., Fellner, P., Gabčová, J., & Sýkorová, A. (2005). Chemical reactions of sulphur species in cryolite-based melts. *Chemical Papers.* 59, 235-239.

[23] Gyarmati, G., Fegyverneki, Gy., Mende, T., & Tokár, M. (2019). The effect of fluxes on the melt quality of AlSi7MgCu Alloy. *International Journal of Engineering and Management Sciences (IJEMS).* 4(1), DOI: 10.21791/IJEMS.2019.1.46.